Nuclear Instruments and Methods in Physics Research A 768 (2014) 104–111

Contents lists available at ScienceDirect

Nuclear Instruments and Methods in Physics Research A

journal homepage: www.elsevier.com/locate/nima

High-precision gas gain and energy transfer measurements in Ar–CO_2 mixtures

Özkan Şahin [a,*], Tadeusz Z. Kowalski [b], Rob Veenhof [a,c]

[a] Department of Physics, Uludağ University, 16059 Bursa, Turkey
[b] Faculty of Physics and Applied Computer Science, AGH University of Science and Technology, Kraków, Poland
[c] RD51 collaboration, CERN, Genève, Switzerland

ARTICLE INFO

Article history:
Received 31 May 2014
Received in revised form
20 September 2014
Accepted 23 September 2014
Available online 2 October 2014

Keywords:
Gas detectors
Penning transfer
Excited states
Photon feedback

ABSTRACT

Ar–CO_2 is a Penning mixture since a fraction of the energy stored in Ar $3p^5 3d$ and higher excited states can be transferred to ionize CO_2 molecules. In the present work, concentration and pressure dependence of Penning transfer rate and photon feedback parameter in Ar–CO_2 mixtures have been investigated with recent systematic high-precision gas gain measurements which cover the range 1–50% CO_2 at 400, 800, 1200, 1800 hPa and gas gain from 1 to 5×10^5.

1. Introduction

Direct ionization of the gas atom can be described with Townsend mechanism:

$$e^- + A \rightarrow e^- + e^- + A^+ \quad (1)$$

where A is the atom on its ground level and A^+ is the ionized atom. In some gas mixtures, apart from the Townsend ionization mechanism, a number of phenomena take place which can significantly contribute to the growth of the electron avalanche. Excitations of the noble gas atoms to metastable A^m or to resonance levels A*, during the avalanche formation, have particular importance for such electron enhancements:

$$e^- + A \rightarrow e^- + A^m \quad (2)$$

$$e^- + A \rightarrow e^- + A^*. \quad (3)$$

When the energies of the excited states are higher than the ionization potential of the admixture (quenching) gas, additional electrons may be released, in the collisions of the excited atoms with the molecules or atoms of the quenching agent, mainly by the following mechanisms:

$$A^m + B \rightarrow A + B^+ + e^- \text{(Penning transfer)} \quad (4)$$

$$A^* + B \rightarrow A + B^+ + e^- \text{(non−metastable Penning transfer)} \quad (5)$$

where B and B^+ are the atoms or molecules and the ionized atoms or molecules of the quenching agent, respectively. It is therefore possible to transfer the energy stored in excited states of one gas component to ionize the other gas in the mixture. These excitation induced ionizations are called “Penning transfers” and the effect of such transfers on gas gain is named as “Penning effect” after Frans Michel Penning who reported on the phenomenon in 1940 [1]. He noticed that the discharge potential in pure noble gases is higher than in their mixtures [2,3].

In a cylindrical counter, the multiplication starts very close to the anode, normally at a few wire radii. So, the detector volume can be divided into two parts: the volume of electron multiplication (M) and the electron drift region (D). In this situation there are four different cases (a, b, c, d) of the production of the additional electrons see Fig. 1 [4,5].

Case a: The additional electrons are created in the same place in which the excited atoms are produced. The effect of these electrons on gas gain is therefore exactly the same as those generated in the Townsend ionization mechanism (impact ionization).

Case b: Extra electrons are generated in some distance from the production point of excitations but in the multiplication volume (M) again. In the cylindrical counter, the electrical field is strongly nonuniform so, the mean multiplication factor for these electrons is smaller than those released in the location of impact ionization region. Both cases a and b

* Corresponding author.
E-mail address: osahin@uludag.edu.tr (Ö. Şahin).

http://dx.doi.org/10.1016/j.nima.2014.09.061
0168-9002/

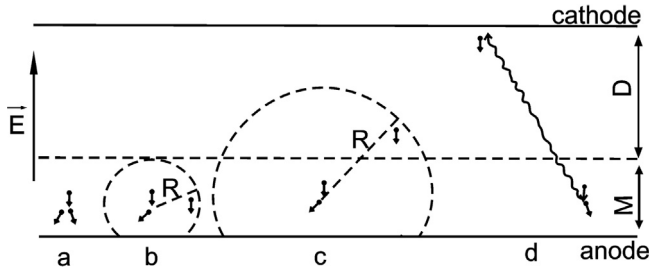

Fig. 1. Simplified diagram for the production of additional electrons. R is the average distance from excitation place to the place of additional electron production.

are required an adjustment on the Townsend coefficient (α) for the Penning transfers (see Section 3.2).

Cases c and d: The extra electrons are created in drift region (D) or on the cathode surface. These electrons are fully multiplied while traveling to the anode wire. Their contributions in the growth of the electron avalanche are seen as over-exponential increases of gas gain curves and can be described by the second Townsend ionization coefficient.

Ar-CO_2 mixture, in varying mixing proportions, have been widely used in gas-based detectors [6–8]. The electron drift velocity and diffusion of these mixtures have been accurately measured [9–11]. In contrast, the gas gain up to now has been accurately measured only for the limited range of CO_2 concentrations: 5%, 10%, 15% and 20% at 1070 hPa [12]. In our earlier work [13], these experimental gas gain curves were fitted with the usage of Magboltz [14] simulation program to determine the contribution of the Penning effect in the avalanche growth. The calculated Penning transfer rates were modeled to identify excitation induced ionization mechanisms. However, extrapolating the transfer rate beyond 20% CO_2 or for lower than 5% CO_2 leads to large uncertainties.

Fortunately, the new measurements of gas gain fill the big gap in CO_2 concentration and led us calculate the transfer rate remarkably accurate in the range 1–50% CO_2 at various pressures. In addition, all parameters describing the energy transfer model that we constructed in [13], in particular the radiative term, are now physical. Since Ar–CO_2 is a commonly used gas mixture in Micro-Pattern Gaseous Detectors (MPGDs) like GEM and MICROMEGAS [15], the updated results obtained in this work are important both for better understanding of their physical properties and for improving their performances.

2. Gas gain measurements

We have measured the gas gain over the range 1–5 $\times$ 10^5 in cylindrical chambers with Ar–CO_2 mixtures at room temperatures. Our tubes have a cathode radius $r_c = 1.25$ cm and a single anode wire with a radius r_a of 24 μm or 50 μm.

We used ^{55}Fe as a radiation source. The source intensity was adjusted to have currents in the range 10 pA–2 nA so as to maintain sensitivity while avoiding space charge. Gas gain G has been determined as the ratio I/I_0, where I and I_0 are the measured current intensities at constant intensity of the incoming photons of X-rays for the applied voltage and for the ionization chamber regime, respectively. A special grid of guard rings protecting the anode has been constructed to minimize the errors on I_0 and on the dark current. The current measurements were performed by a Keithley 6485 pm with resolution of 10 fA. Argon of purity 5.0 and CO_2 of purity 4.8 were used in the measurements. For the pressure measurements and gas mixture preparation SETRA Model 280E Pressure Transducer with the resolution of 0.1 mBar is used. Uncertainties for the gas mixture preparations were less than 1%; the admixture concentration was defined as fraction of the partial pressure of CO_2 to the total pressure of the mixture (p_{CO_2}/p_{gas}). Therefore, the error of the measured gas amplification factor is only limited by the uncertainties on I_0 with 2.5% and I with 2% for different voltages. Consequently, the absolute accuracy of the gas gain to be better than 5% has been reached.

Some measurements were repeated few times to check the reproducibility. The difference in the values of gas gain was always much below than 1%. Typical gas gain curves measured in Ar 50%-CO_2 50% mixtures at 0.40, 0.79, 1.19 and 1.78 atm are shown in Fig. 2, as an example.

3. Data analysis method

There are two fit parameters that we have extracted from the fits of the gas gain measurements:

- Penning transfer rate, the fraction of excitation-induced ionizations, is the main parameter that we have to determine from each measured gas gain curve.
- When there is an over-exponential growth on gas gain curve, it is not possible to reproduce the whole curve using only Penning term. In such a case one more free fit parameter is needed to describe photon feedback effect on the gas gain.

Since we do not a priori know the Penning transfer rates, we have developed a tool to derive them from the gas gain measurements. The tool first reads the measured gas gain data and the output file of Magboltz software [14]. Then, it proceeds a numerical integration of the Townsend coefficients written in the Magboltz output file to simulate gas gain (see Section 3.2).

A fitting procedure has been added into the our simulation program which iterates using a non-linear least squares method to find both the transfer rates and photon feedback parameters (if necessary). The fit program returns the errors on the fit parameters and the covariance matrix which are needed not only to

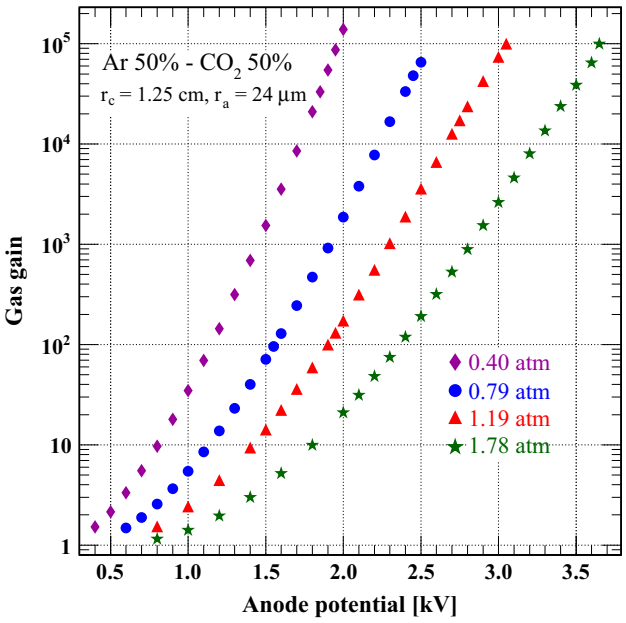

Fig. 2. Measured gas gain curves for the highest CO_2 percentage considered in this work.

check reliability of the results but also essential to construct proper models from them (see Sections 4.1 and 4.4).

3.1. Magboltz software

The Magboltz [14] code performs a Monte Carlo simulation to compute the transport properties of electrons in the gas by solving the Boltzmann transport equation. The program use excitation, ionization, attachment, elastic and inelastic scattering cross-sections to determine collision parameters with a random generator while tracking the electrons step by step under the influence of the electric field.

The input file of the program consists of electric and magnetic field, gas pressure and temperature, the fractions of the each gas type in the mixture. The output file contains all needed transport parameters for the gas gain fits such as Townsend coefficients α, collision frequencies (production rates) of excitations and ionizations with varying electric field strengths in the given range.

In this work Magboltz 9.0.1 version is used for the gas gain simulations. The excitation rates for 44 different levels of argon can be computed with this version. Although there are infinite number of excitations located below ionization threshold of argon (15.76 eV), the number of levels handled by this version is sufficient for our purpose to calculate the Penning transfer rates.

3.2. Penning adjustment

The gas gain G including Penning adjustment for a single wire tube can be written as

$$G = \exp \int_{r_m}^{r_a} \alpha_{Pen} E(r)\, dr \tag{6}$$

here, r is the radial distance from the anode wire, r_m is the starting point of the multiplications ($\alpha > 0$, α is the Townsend coefficient), r_a is the radius of the anode wire and $E(r)$ is the electric field at point r for the given voltage. The compact form of the excitation induced (adjusted) Townsend coefficient α_{Pen} is defined with the following expression (also see [13]):

$$\alpha_{Pen} := \alpha\left(1 + r_{Pen}\frac{f^{exc}}{f^{ion}}\right), \tag{7}$$

where,

f^{ion}: the total frequencies (production rates) of the direct ionizations (Ar^+ and CO_2^+),

f^{exc}: sum of the production rates for the excited argon states which have larger energy than the ionization threshold of CO_2 (13.77 eV),

r_{Pen}: Penning transfer rate, the probability that an excited argon atom ionizes a CO_2 molecule.

In the calculations, it is assumed that f^{ion} is proportional to α. The production rates of the first lowest argon excited states ($3p^5 4s$), located at 11.55 eV (metastable), 11.62 eV (resonance), 11.72 eV (metastable) and 11.83 eV (resonance), are not taken into account in the fits as their energies are below ionization threshold of CO_2. We assume the same value of r_{Pen} probability for all excited argon levels while fitting the measured gas gain curves.

In consequence, Penning transfer rates in Ar–CO_2 mixtures are determined as the fraction of the $3p^5 3d$ and higher argon excited states that needs to be added to the Townsend coefficient α.

3.3. Photon feedback

If the excited argon atoms (Ar^*) and excimers (Ar_2^*, see Section 4.1) cannot dissipate their excess energy via inelastic collisions, then they will decay under photon emission. Radiative states which decay directly to the ground emits VUV photons. If such photons are not able to be stopped in the quencher gas (CO_2) sufficiently, then they may reach to the cathode surface at where they can create photo-electrons since they have bigger energy than the work function of the cathode metal. The radiative photons emitted from $3p^5 3d$ and higher argon excited states are also capable of ionizing CO_2 molecules. The additional electrons, produced far from the main avalanche region, will develop their own avalanches. These secondary avalanches give an over-exponential increase in the gas gain curve (called photon feedback).

Photon feedback can be described with a single parameter β which is the number of secondary avalanches created by one avalanche electron [16]. If the gas gain without feedback is G, then the gas gain enhancement in the first generation will be βG^2 which creates $\beta^2 G^3$ electrons in the second generation. Over several generations of such gas gain enhancements, the total number of avalanche electrons G_T at anode can be written as

$$G_T = G + \beta G^2 + \beta^2 G^3 + \cdots = \frac{G}{1-\beta G} \tag{8}$$

A breakdown occurs in the counter when $\beta G \approx 1$, which is known as a stability condition for the counters.

The Penning transfer rate r_{Pen} is not strongly correlated with β so, we could separate these parameters while fitting the measured gas gain curves.

4. Outcome of data analysis

Typical example of the gas gain fits for Ar 99% - CO_2 1% mixture at various pressure is shown in Fig. 3. The red circles are the measured gas gain data; the error bars are smaller than the markers. Dashed lines show the calculated gas gain curves without any corrections. Thin straight lines are the fits extracted from Penning adjusted Townsend coefficients; but photon feedback parameters are not taken into account in these fits. Thick straight lines are the final fit results including both Penning adjustment

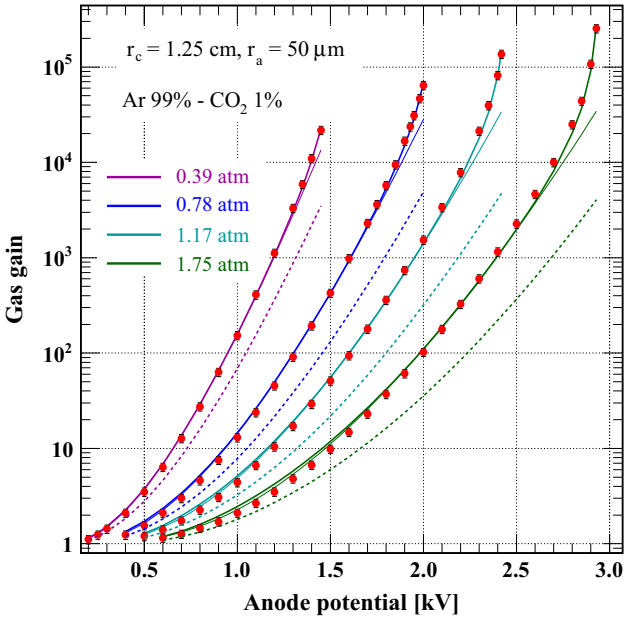

Fig. 3. Calculated and measured gas gain curves for the lowest CO_2 percentage considered in this work. Dashed lines—calculated without any corrections; thin straight lines—Penning transfer included; thick straight lines—both Penning transfer and photon feedback included; points—measured data.

and photon feedback correction. The same fitting procedures were repeated for each mixture set of the measured gain curves at different pressures to determine the Penning transfer rate (r_{Pen}) and photon feedback parameter (β). Such obtained r_{Pen} and β parameters are analyzed in next sections of this paper.

4.1. Parametrization of the Penning transfer rates

As seen from Fig. 4, the energy transfer rate (r_{Pen}) always increases with the CO_2 concentration at the same gas pressure. This is simply result of the decreasing time between collisions of the excited argon atoms with quencher molecules (CO_2). The lifetime of the argon excited states remains constant and they find greater number of recipients around for Penning transfers at higher percentages of CO_2 in the mixture.

Pressure dependence of the transfer curves for 1% CO_2 and 2% CO_2 mixtures can be described with a two parameter fit function [13]:

$$r_{Pen}(p) = \frac{b_1 p}{p + b_2} \tag{9}$$

here, p dimensionless pressure is related to the gas pressure by $p_{gas} = p \times 1$ atm, b_1 indicates the asymptotic value of the energy transfer and b_2 gives the collisional energy transfer efficiency ($Ar^* + CO_2 \rightarrow Ar + CO_2^+ + e^-$).

At higher concentrations than 2% CO_2, r_{Pen} initially rises with increasing pressure for the same reasons as the rise with concentration. The transfer rates reach their maximum at 1.2 atm for the mixtures with 4% of CO_2 and more. Surprisingly, there are hints that the transfer rate actually drops at the highest pressures for the same CO_2 fraction. Such a drop indicates the processes by which excited argon atoms (Ar^*) are lost. For instance, excited argon molecule formations (Ar_2^*, argon excimer) lead destruction of Ar^* by the following process:

$$Ar^* + Ar + Ar \rightarrow Ar_2^* + Ar. \tag{10}$$

Argon excimers can decay by emitting VUV photons:

$$Ar_2^* \rightarrow Ar + Ar + \gamma. \tag{11}$$

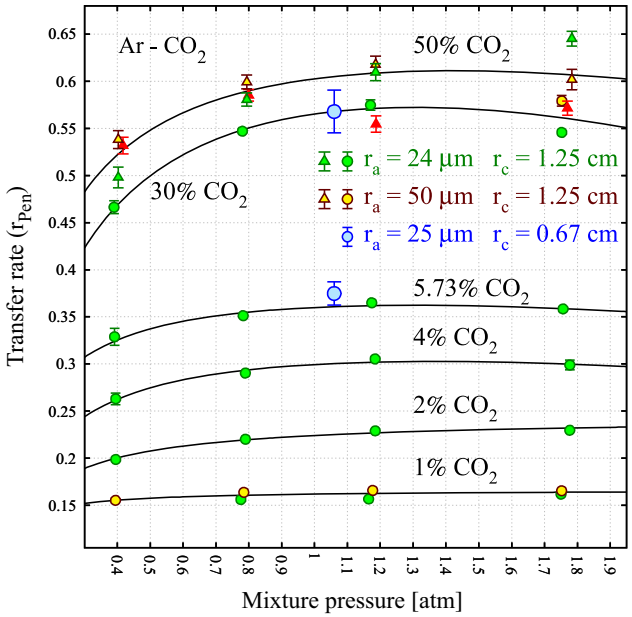

Fig. 4. Energy transfer probabilities extracted from gas gain curves for different counters parameters as the function of mixture pressure. The probabilities for 50% CO_2 mixtures are shown with triangles to be distinguished from those for 30% CO_2 mixtures. For comparison, data from [13] (the two blue circles) are also given. The transfer curves lines are fitted by Eq. (9) or Eq. (14). (For interpretation of the references to color in this figure caption, the reader is referred to the web version of this article.)

They can also excite and ionize some quencher molecules (B):

$$Ar_2^* + B \rightarrow Ar + Ar + B^* \tag{12}$$

$$Ar_2^* + B \rightarrow Ar + Ar + B^+ + e^-. \tag{13}$$

The highest energy level of argon excimers stay in "first continuum" which have a peak at 11.3 eV [17]. Because of the high ionization potential of CO_2 (13.77 eV) none of the argon excimers have capable of ionizing CO_2 molecules through the photo-ionization, nor with the mechanism given in Eq. (13). If decayed photons from the argon excimers cannot be absorbed efficiently in CO_2 then may reach the cathode and initialize secondary avalanches by extracting photo-electrons from the surface, the process described by β factor (see Eq. (8)). Therefore, they are thought to be a source of photon feedback when the Penning transfer losses its competency in Ar–CO_2 mixtures.

Since the excimers develop in a three-body interaction [18,19], the process is proportional to the square of the gas pressure. So, the Ar_2^* formation become increasingly likely with increasing pressure [20]. Under these considerations we have found that the reduction of the transfer rate at the highest pressure can be modeled with a b_3 parameter:

$$r_{Pen}(p) = \frac{b_1 p}{p + b_2} + b_3 p^2 \tag{14}$$

The fit parameters, obtained from the present systematic gas gain measurements, are given in Table 1 with their errors.

4.2. Transfer curve at atmospheric pressure

Concentration dependence of the transfer rate shown in Fig. 5 was defined by the following fit function (also given in [13]):

$$r_{Pen}(f_q) = \frac{a_1 f_q + a_3}{f_q + a_2} \tag{15}$$

where f_q is the fraction of CO_2, the parameter a_1 is the asymptotic transfer rate and a_3/a_2 ratio gives the ionization probability of CO_2 by the decayed photons (γ) from Ar $3p^5 3d$ and higher states:

$$Ar^* \rightarrow Ar + \gamma$$
$$\gamma + CO_2 \rightarrow CO_2^+ + e^- \tag{16}$$

The Penning transfer rates shown with the blue circles were obtained in [13] using data from [12]. The green circles represent the transfer rates extracted from the present gas gain measurements. Their values at 1070 hPa are calculated using either Eq. (9) or Eq. (14) with the fit parameters listed in Table 1. The updated transfer curve with green line is derived from Eq. (15) by taking into account both data from [13] and the recent transfer rates. Error propagation is applied, using covariance matrix of the fit results, to determine uncertainties (green error band).

Thanks to the recent gas gain measurements large uncertainty on the transfer curve beyond 20% CO_2 is considerably decreased. In addition, the recent rates obtained from 5.73% CO_2 and lower CO_2 concentrations have the highest accuracy. Extrapolation of the transfer curve to the pure argon gives a positive radiative transfer

Table 1
Fit parameters of the transfer curves shown with lines on Fig. 4.

CO_2 (%)	b_1	b_2	b_3
1	0.1667 ± 0.0031	0.0287 ± 0.0156	–
2	0.2434 ± 0.0032	0.0858 ± 0.0119	–
4	0.3432 ± 0.0179	0.1208 ± 0.0341	-0.0068 ± 0.0044
5.73	0.3999 ± 0.0217	0.0898 ± 0.0398	-0.0070 ± 0.0045
30	0.7046 ± 0.0708	0.1970 ± 0.0786	-0.0235 ± 0.0142
50	0.6974 ± 0.0507	0.1324 ± 0.0488	-0.0134 ± 0.0119

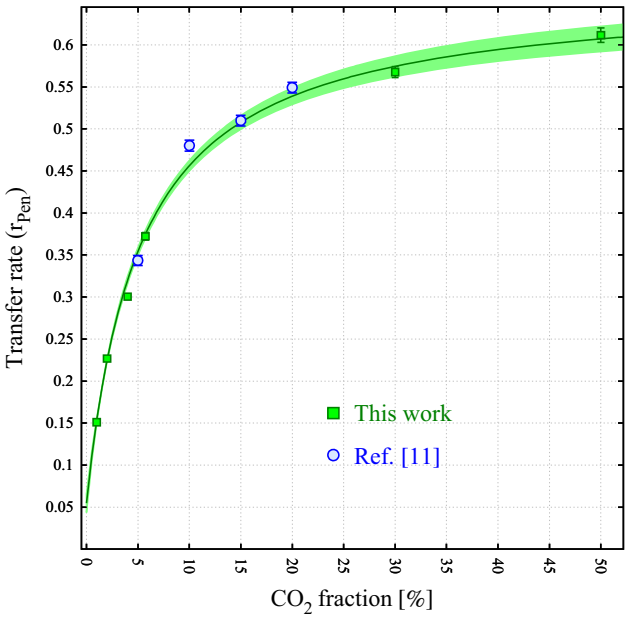

Fig. 5. Transfer rate, r_{Pen}, in Ar–CO_2 as the function of CO_2 concentration at mixture pressure of 1070 hPa. Line is the data fit with Eq. (15).

Table 2
Fit parameters of the transfer curve for Eq. (15).

Parameter	This work
a_1	0.6643 ± 0.0208
a_2	0.0518 ± 0.0056
a_3	0.0028 ± 0.0009

probability ($a_3/a_2 = 0.0541 \pm 0.0183$, see Table 2) for the mechanism represented by Eq. (16).

4.3. Source of the photon feedback

Feedback is expected to be driven by photons from the decay of the Ar $3p^5 4s$ radiative states (11.62 eV and 11.83 eV) because of the following reasons:

- They are the most abundantly produced excited states. For instance, the production rates of the $3p^5 4s$ excitations, in Ar 96% - CO_2 4% mixture, are $\approx 2-4$ times larger than the rates of the second most abundant states ($3p^5 3d$, 13.86 eV) at 100 kV/cm electric field strength (see Fig. 6).
- They cannot be lost in Penning transfers since their energies are lower than the ionization potential of CO_2 molecules (13.77 eV). So, they will either be absorbed by CO_2 without producing additional electrons or will reach the cathode surface at where they can initialize secondary electrons by photoelectric effect.
- The photo-absorption cross-section of CO_2 (σ_{pa}) for these states is low among the other most produced excited states of argon ($3p^5 3d$ and $3p^5 5s$), as seen on Fig. 7. Therefore, the photons emitted from argon $3p^5 4s$ levels are more likely to be absorbed at large distances from the wire or to reach the cathode.

The mean free path of photons $\lambda_{ph}(\epsilon)$ can be calculated using the photo-absorption cross-section of the quencher (CO_2):

$$\lambda_{ph}(\epsilon) = \frac{1}{n f_q \sigma_{pa}(\epsilon)} \tag{17}$$

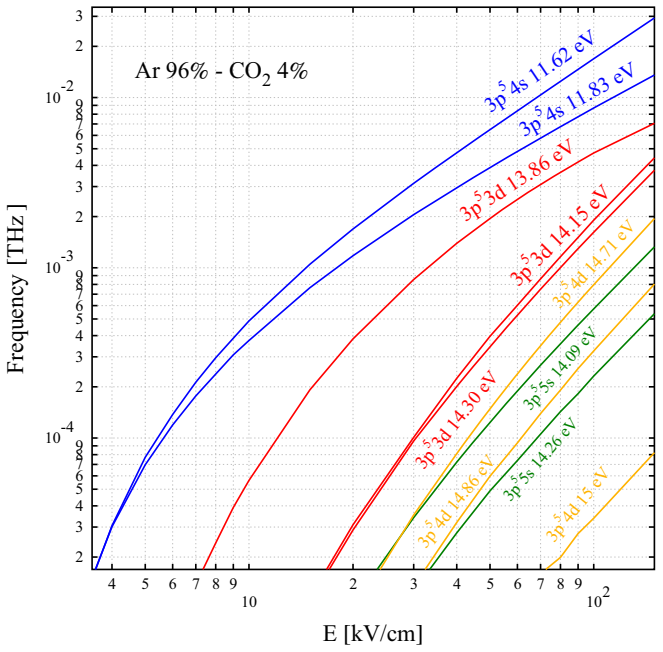

Fig. 6. Production rates of argon excited states that can decay to ground under photon emission, calculated with Magboltz 8.9.1 for 300 K temperature at 1 atm as the function of electric field strength.

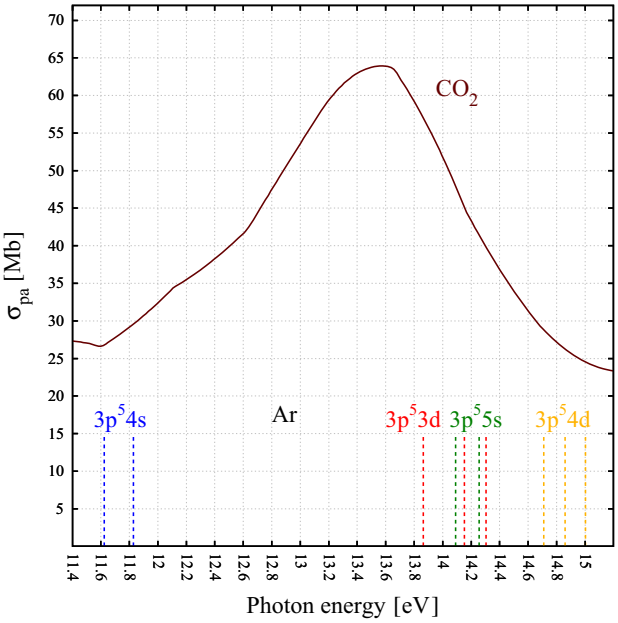

Fig. 7. Photo-absorption cross-section of CO_2, from Berkowitz [21] and references therein. The dashed lines mark the energies of argon radiative states.

where ϵ is energy of the photon and f_q is concentration of the quencher in the mixture. The number density of the gas is given by:

$$n = \frac{p_{gas}}{k_B T_{gas}} \tag{18}$$

here, T_{gas} and k_B are the gas temperature and the Boltzmann constant, respectively. The mean free paths of the argon $3p^5 4s$ de-excitation photons, for Ar–CO_2 mixtures (1–50% CO_2) at various pressures, are shown in Fig. 8.

The avalanche size r_{size} is, along with the mean free path of photons, an essential parameter in order to identify contributions of the radiative photons in multiplications. It is a measure of the

region in which an electron attains sufficient energy from the applied field to ionize other gas atoms or molecules between the collisions while moving to the anode. This parameter, for a single wire cylindrical counter, can be obtained using both gas gain measurements and the Townsend coefficient α computed by Magboltz program:

$$r_{\text{size}} = \frac{V_{\text{avl}}}{E_{\text{avl}} \log(r_c/r_a)} \tag{19}$$

here, the electric fields (E_{avl}) at where $\alpha = 1$ [1/cm] are extracted from the Magboltz data. The avalanche potentials (V_{avl}) are the values of bias voltages for a selected values of gas gain for which the avalanche size is calculated. For the pressure dependence of the avalanche size, the lower and upper limit of the gas gain is chosen as 80 and 8000, respectively. The corresponding avalanche potentials for these gas gain limits are determined from the experimental gas gain curves.

In Fig. 8, the top edge of the avalanche size is defined by the upper limit of the gas gain. We do not choose larger gas gain than 8000 since maximum of the gas gain e.g. measured in the tube with $r_a = 24$ μm anode wire radius for 1% CO_2 at 1.75 atm mixture pressure is below the gas gain of 10^4 (see Fig. 9).

The bottom edge of the avalanche size corresponds to the lower limit of gas gain. So, the selection of gas gain larger than 80 does not change the process of avalanche growth if the photons are absorbed inside the multiplication region (avalanche size). This is the case in the mixtures with 5.73%, 30% and 50% CO_2 (see Fig. 8). It is important to identify the non-efficiency of the photon absorptions in the multiplication region, in the size of electron avalanche. The absorption of these photons in the area of electron multiplication leads to modification of the Townsend coefficient α, do not contribute to photon feedback. It is expected from the $1-\beta G$ denominator of Eq. (8) that for small gas gain the effect of the photon feedback on gas gain becomes insignificant. Therefore, we do not calculate the avalanche sizes for smaller gas gain than 80.

The mean free path for argon $3p^5 4s$ de-excitation photons in the 1% CO_2 mixture at 0.4 atm is ≈ 4 mm (see Fig. 8). This distance is three times smaller than the cathode radius ($r_c = 1.25$ cm). However,

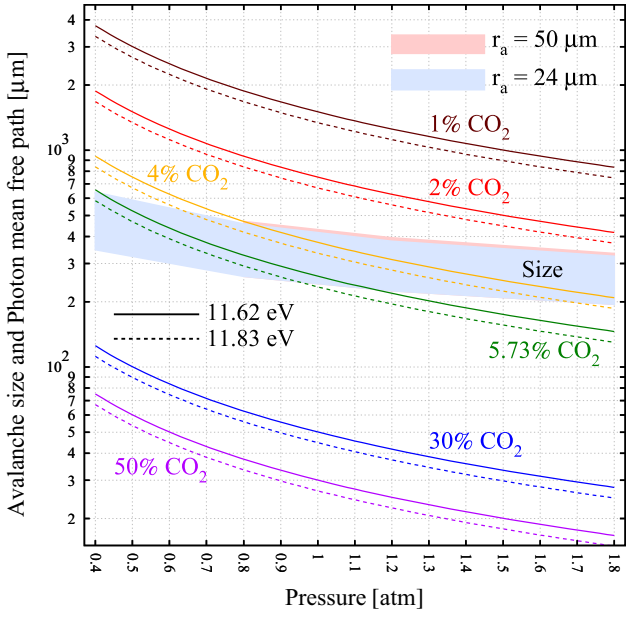

Fig. 8. Mean free path of the photons (lines) emitted from argon $3p^5 4s$ radiative states and the avalanche sizes between the gas gain of 80 and 8000. The mean free paths and the sizes are calculated from Eqs. (17) and (19), respectively, as the function of mixture pressure.

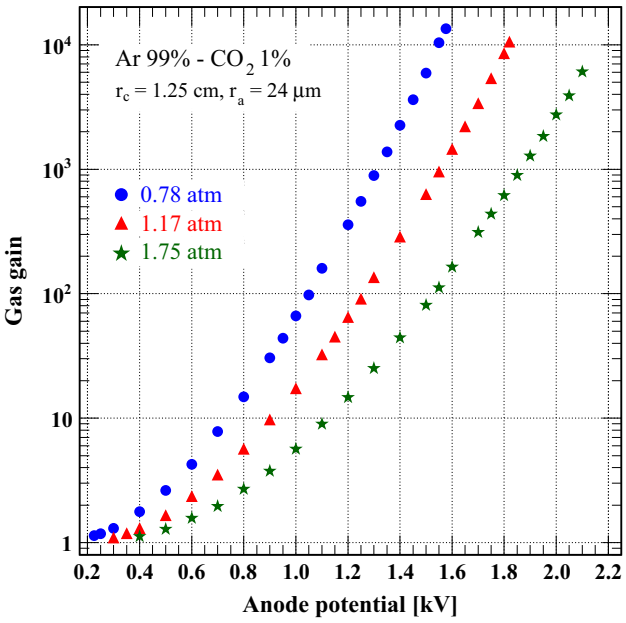

Fig. 9. Measured gas gain curves in tube with $r_a = 24$ μm anode wire radius at various mixture pressures.

they can still arrive the cathode surface and produce free electron as their energy is higher than the working function of cathode material. The photons emitted from Ar $3p^5 3d$ and higher radiative states, having smaller frequency of excitation (see Fig. 6), can also contribute in production of additional electron with photo effect from the cathode or in the process (16). The probability of the photo effect from the cathode is higher for the mixtures with low CO_2 percentages at low pressures. Some higher excited levels of argon can decay eventually to the $3p^5 4s$ states. If this mechanism is emerged in the drift region then the probability that $3p^5 4s$ de-excitation photons reach to the cathode will increase thus increasing the number of extra electrons.

Concentration dependence of the avalanche sizes between the gas gain of 2000 and 8000 in tubes which have a single anode wire with radius r_a of 24 μm (bands) and of 50 μm (circles and triangles) are shown in Fig. 10. There are limited number of gas gain data measured in the tube with $r_a = 50$ μm anode wire (1%, 30%, 50%, 50.2% CO_2). Dashed lines are drawn to guide the eye to compare these avalanche sizes with the avalanche sizes calculated for $r_a = 24$ μm tube. The gas gain of 2000 corresponds to the bottom edges of the bands and the triangles while the upper bands and the circles are calculated for the gas gain of 8000 on Fig. 10.

4.4. Photon feedback parameters

The photon feedback parameters β are determined from the fits using Eq. (8) (see Section 3.3) to describe over-exponential increases on the measured gas gain curves. Interpretations of the feedback parameters here are mostly based on the discussions given in Section 4.3.

At 0.4 atm the photon feedback parameter β is flat (Fig. 11) for the mixtures with low CO_2 percentages (1–5.73%) in which photo-ionization occurs at a larger distance than the avalanche size (see Fig. 8). This refers that most of the de-excitation photons arrive the cathode and the foto-electrons extracted from the surface are fully multiplied.

It is seen on Fig. 11 that the feedback parameters obtained from the gas gain measurements in the tube with $r_a = 50$ μm anode wire (circles) are larger than calculated for the tube with thinner anode wire ($r_a = 24$ μm). The following arguments can be proposed to

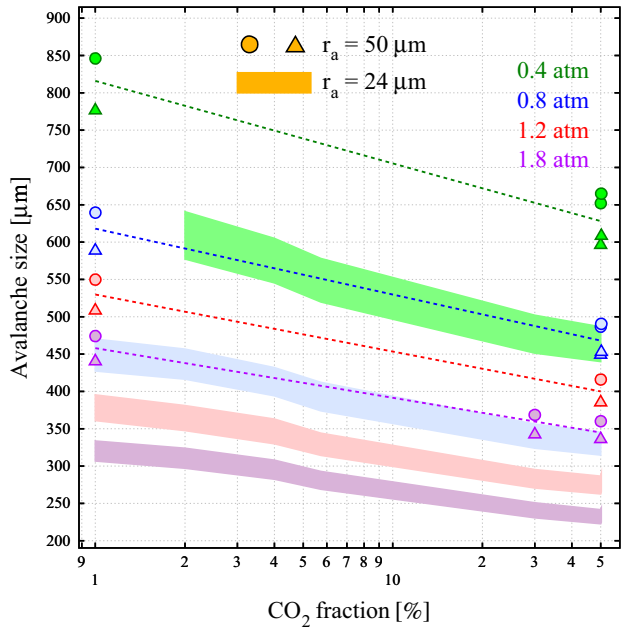

Fig. 10. Avalanche sizes in varying CO_2 concentrations for the tubes with different anode wire radii used in gas gain measurements. The triangles and circles correspond to the gas gain of 2000 and of 8000, respectively. Dashed lines to guide the eye. Calculated from Eq. (19).

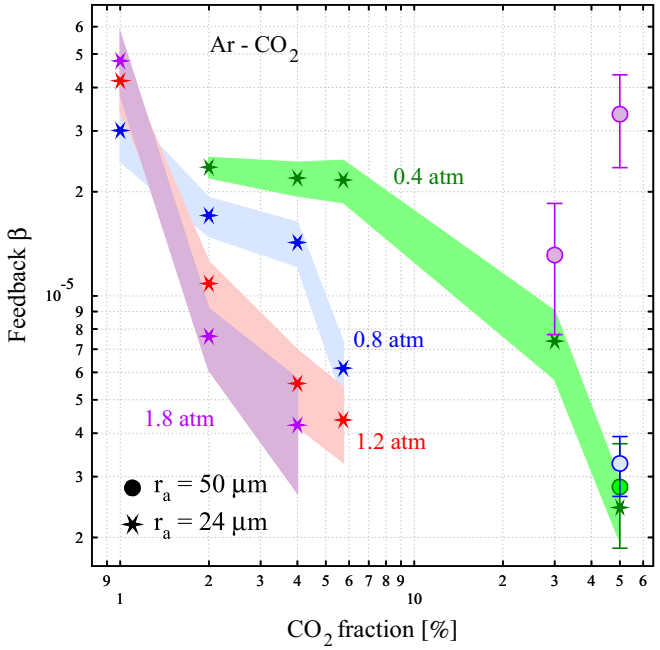

Fig. 11. Concentration dependence of the feedback parameter β. Extracted from the experimental data to fit over-exponential increases of the gas gain curves. Precision of the parameters is shown by bands and bars.

explain this: Excited argon atoms are not always subjected to collisional (Eq. (5)) or to radiative (Eq. (16)) Penning transfers, even tough they are energetically eligible to ionize CO_2 molecules. Due to dependence of electrical field distribution on the anode radius, the excited Ar $3p^5 3d$ states and higher levels are created on average far from the anode wire for higher radius of anode, so the decayed photons from these states are created more closely to cathode. Their absorption by the quencher (CO_2) is smaller since the distance of the avalanche to the cathode is shorter compared to the tube with thinner wire (see Fig. 10).

In the 1% CO_2 mixture, β increases with the pressure (beyond 0.8 atm), for both anode wire radii (Fig. 12), although escape probability of the photons from the avalanche region decreases with the pressure (Fig. 8). This indicates two arguments:

- Not only photon feedback causes over-exponential growth of the gas multiplication, but also other processes, e.g. argon ions arriving at cathode, may contribute to the feedback (ion feedback). Such a case is independent of the quencher (CO_2) fractions, but rather has a dependence on the electric field strength which becomes higher with increasing pressure to achieve the same gas gain.
- Alternatively, de-excitation photons emitted from argon excimers can contribute to the cathode feedback as mentioned in Section 4.1. They cannot be absorbed efficiently by CO_2 molecules as a consequence of low absorption cross-section in this low admixture concentration. Pressure square growth of this process also supports the increasing trend of the feedback parameters (see the explanations for Eq. (14)).

Probability of the escaping photons from the main avalanche region in which multiplication starts is higher in tubes with thinner anode radius since the avalanche is held in a narrower region (see, the bands and the dashed lines on Fig. 10). In 1% CO_2 mixtures, β is therefore larger for the tube with $r_a = 24$ μm than found in $r_a = 50$ μm (see the green band and the green circles shown in Fig. 12).

Feedback decreases with pressure in the 2%, 4% and 5.73% CO_2 mixtures and the drop is steeper for the higher CO_2 concentrations (Fig. 12). This reflects the reduction of the mean free path of photons emitted by the argon excited states. A smaller mean free path will lead to less secondary gas gain since the probability that the photons undergo radiative transfers inside the main amplification zone increase. In this situation, secondary avalanches initialized by the photons will seem like a Penning enhancement on the gas gain curves rather than leading an over-exponential growth.

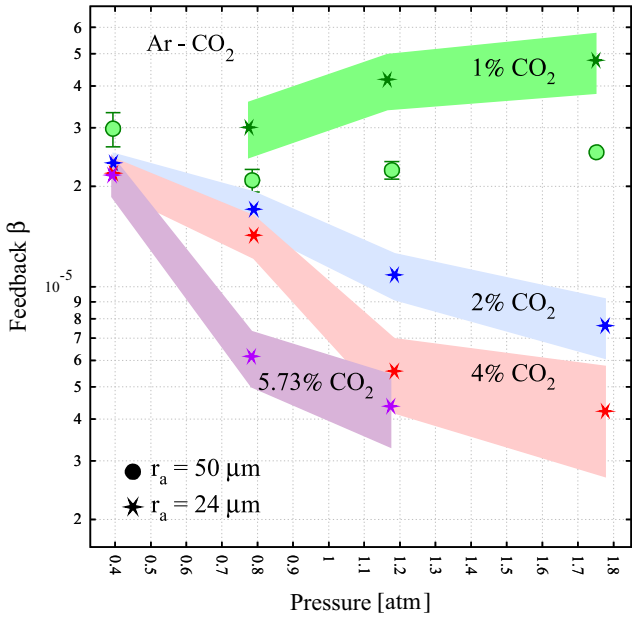

Fig. 12. Feedback parameter β versus gas pressure in the range of 1–5.73% CO_2 fraction, extracted from the gas gain curve fits.

5. Conclusions

Excitation induced ionization mechanisms have been investigated using high precision gas gain data measured in single wire cylindrical proportional counters filled with $Ar-CO_2$ mixtures at various pressures. The Penning transfer rates and the photon feedback parameters, contributions of the excited argon atoms to the direct ionizations, have been extracted from the recent systematic gas gain measurements.

The reductions of the transfer rate at the highest pressures indicate excimer formations in which excited atoms are lost with three-body interactions. The energy transfer model has been developed so that describes diminish of the transfer rates.

The transfer rates obtained from the recent measurements confirm existing transfer data in the literature [13].

The feedback parameters have been justified with the photon mean free path and the avalanche size. It is noticed that the main feedback source is expected to be Ar $3p^5 4s$ radiative states. There are evidences in some cases that argon excimers, high level de-excitation photons and ions are other potential sources for the cathode feedback processes.

Acknowledgments

This work was funded by the Turkish Atomic Energy Authority (2013 TAEK CERN-A5.H2.P1.01-23) and supported partially by the Polish National Science Centre, grant no. DEC-2013/10/M/ST7/00568.

References

[1] M.J. Druyvesteyn, F.M. Penning, Reviews of Modern Physics 12 (1940) 87, Erratum: Rev. Mod. Phys. 13 (1941) 72.
[2] F.M. Penning, Z Physics 46 (1928) 335.
[3] F.M. Penning, Physica 1 (1934) 1028.
[4] K. Jeleń, Avalanche multiplication of electron in the mixtures of gases and vapours, Scientific Bulletins of the Stanislaw Staszic University of Mining and Metallurgy, No 786, Craców 1980 (in Polish).
[5] J. Zajac, Electron multiplication process in the mixtures of gases and vapours at low mixture pressure (Ph.D. thesis), AGH, University of Science and Technology, Craców, Poland, 1994.
[6] H. Zhan-Ying, et al., Chinese Physics C 38 (2014) 219.
[7] A. Yoshikawa, et al., Journal of Instrumentation 7 (2012) C06006-1.
[8] S. Chakravarty, J.C. Armitage, Nuclear Instruments and Methods in Physics Research Section A 321 (1992) 1.
[9] T. Zhao, et al., Nuclear Instruments and Methods in Physics Research Section A 340 (3) (1994) 485.
[10] P. Colas, et al., Nuclear Instruments and Methods in Physics Research Section A 478 (1–2) (2002) 215.
[11] A. Andronic, et al., Nuclear Instruments and Methods in Physics Research Section A 523 (2004) 302.
[12] T.Z. Kowalski, et al., Nuclear Instruments and Methods in Physics Research Section A 323 (1992) 289.
[13] Ö. Şahin, et al., Journal of Instrumentation 5 (2010) P05002 1–30.
[14] S.F. Biagi, Nuclear Instruments and Methods in Physics Research Section A 421 (1999) 234.
[15] F. Sauli, Nuclear Instruments and Methods in Physics Research Section A 386 (1997) 531.
[16] I. Krajcar Bronić, B. Grosswendt, Nuclear Instruments and Methods in Physics Research Section B 142 (1998) 219.
[17] P. Millet, et al., Journal of Physics B: Atomic, Molecular and Optical Physics 15 (1982) 2935.
[18] T. Oka, et al., The Journal of Chemical Physics 70 (7) (1979) 3384.
[19] W. Wieme, J. Lenaerts, Journal of Chemical Physics 74 (1981) 483.
[20] J. Wieser, et al., Review of Scientific Instruments 68 (1997) 1360.
[21] J. Berkowitz, Atomic and Molecular Photoabsorption, Academic Press, UK and USA, 2002, chapter 5, pp. 189–197.